Supplemental material

Gunawan et al., https://doi.org/10.1083/jcb.201807175

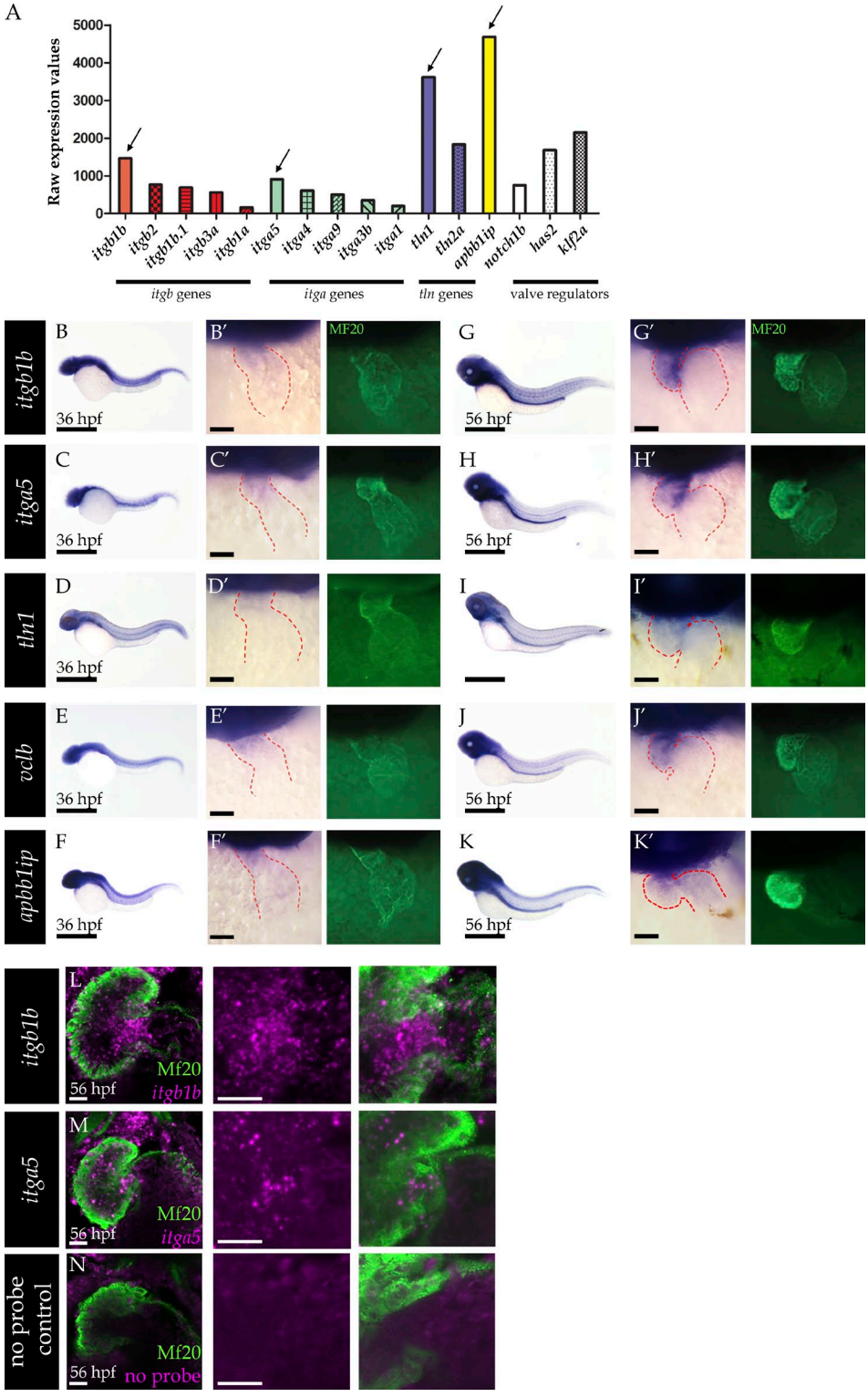

Figure S1. **FA factor gene expression appears enriched in the AVC at the time of AV EC migration.** Related to Fig. 2. **(A)** Expression levels of FA-associated factor genes, as detected by microarray analysis of 52-hpf hearts. Genes encoding FA-associated factors with comparable expression levels to genes encoding known valve regulators (*notch1b*, *has2*, and *klf2a*) are shown. Graph includes the five most highly expressed *itgb* and *itga* genes and *tln1* and *tln2a*, and *apbb1ip* genes. **(B–K′)** Whole-mount in situ hybridization showing *itgb1b* (B and B′ and G and G′), *itga5* (C and C′ and H and H′), *tln1* (D and D′ and I and I′), *vinculin-b (vclb)* (E and E′ and J and J′), and *apbb1ip* (F and F′ and K and K′) expression. (B′–I′) Immunostaining for MF20 (green) labeled the hearts. FA factor genes appeared weakly expressed in the ventricle of 36-hpf hearts (B–F) and more strongly detected in 56-hpf hearts, particularly in the AVC (G–K). Embryos of different developmental stages were processed in the same tubes. **(L–M)** Fluorescence in situ hybridization showing *itgb1b* and *itga5* expression. Expression of *itgb1b* (L) and *itga5* (M) appears enriched in AV ECs. No signal is observed in AV ECs in the negative control (N; secondary antibody treatment without in situ probes). Scale bars: (B–K) 500 µm; (B′–K′) 50 µm; (L–N) 10 µm.

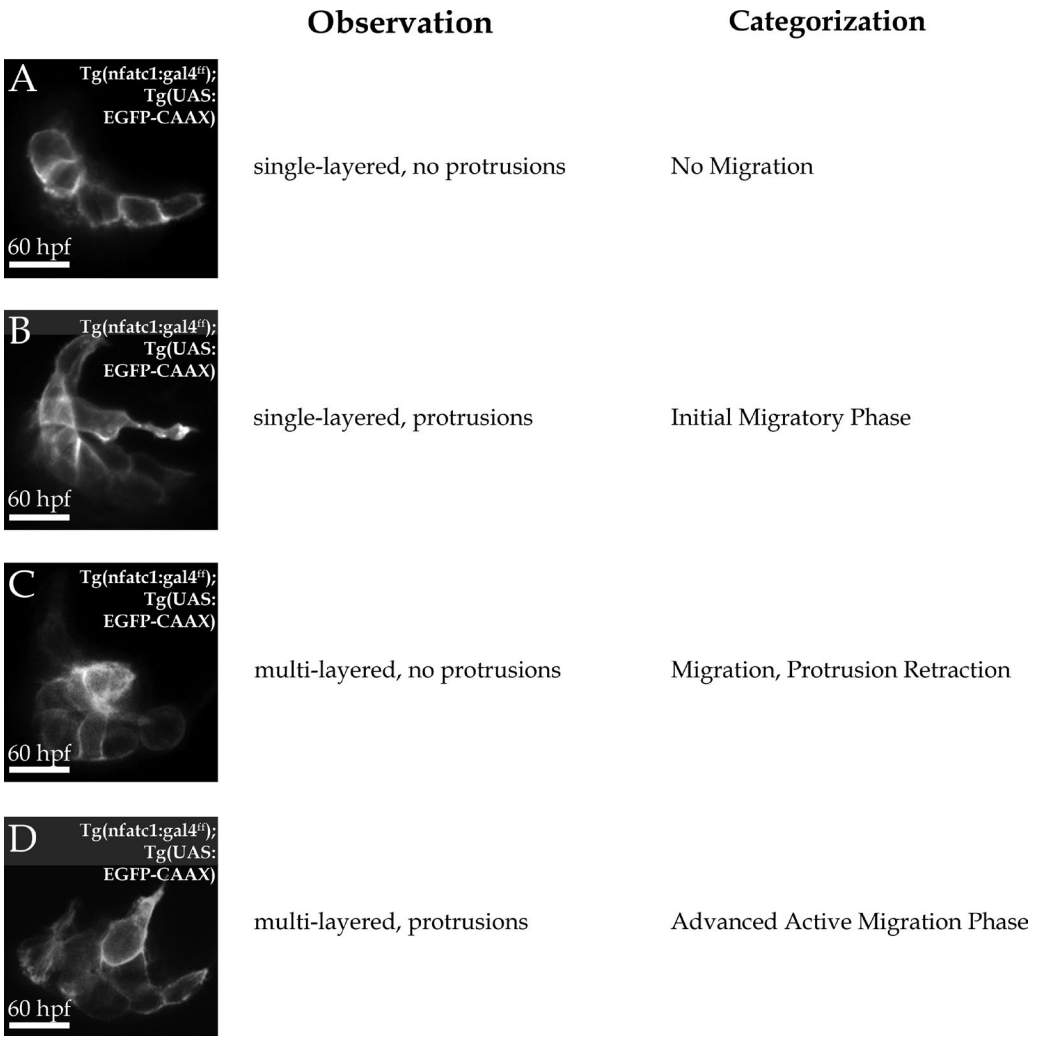

Figure S2. **Characterization of AV EC migration stages.** Related to Figs. 3 and 8. **(A and B)** Single layer of AV ECs, early migratory phase typically observed between 48 and 55 hpf in WT embryos. (A) No migration: AV ECs composed a single layer of cells, with no visible protrusions. (B) Initial migration stage. One to three AV ECs extended protrusions into the ECM. The base of the cell was still in contact with the cardiac lumen. **(C and D)** Multilayered AV ECs, the advanced migratory phase typically observed between 55 and 65 hpf in WT embryos. (C) Migration, retraction phase of protrusions. AV ECs were multilayered, indicating movement into the ECM. No clear protrusions were observed, suggesting that the cells were in the protrusion retraction phase. (D) Advanced migration stage. AV ECs were multilayered, and one to three ECs extended protrusions. Scale bars: 10 µm.

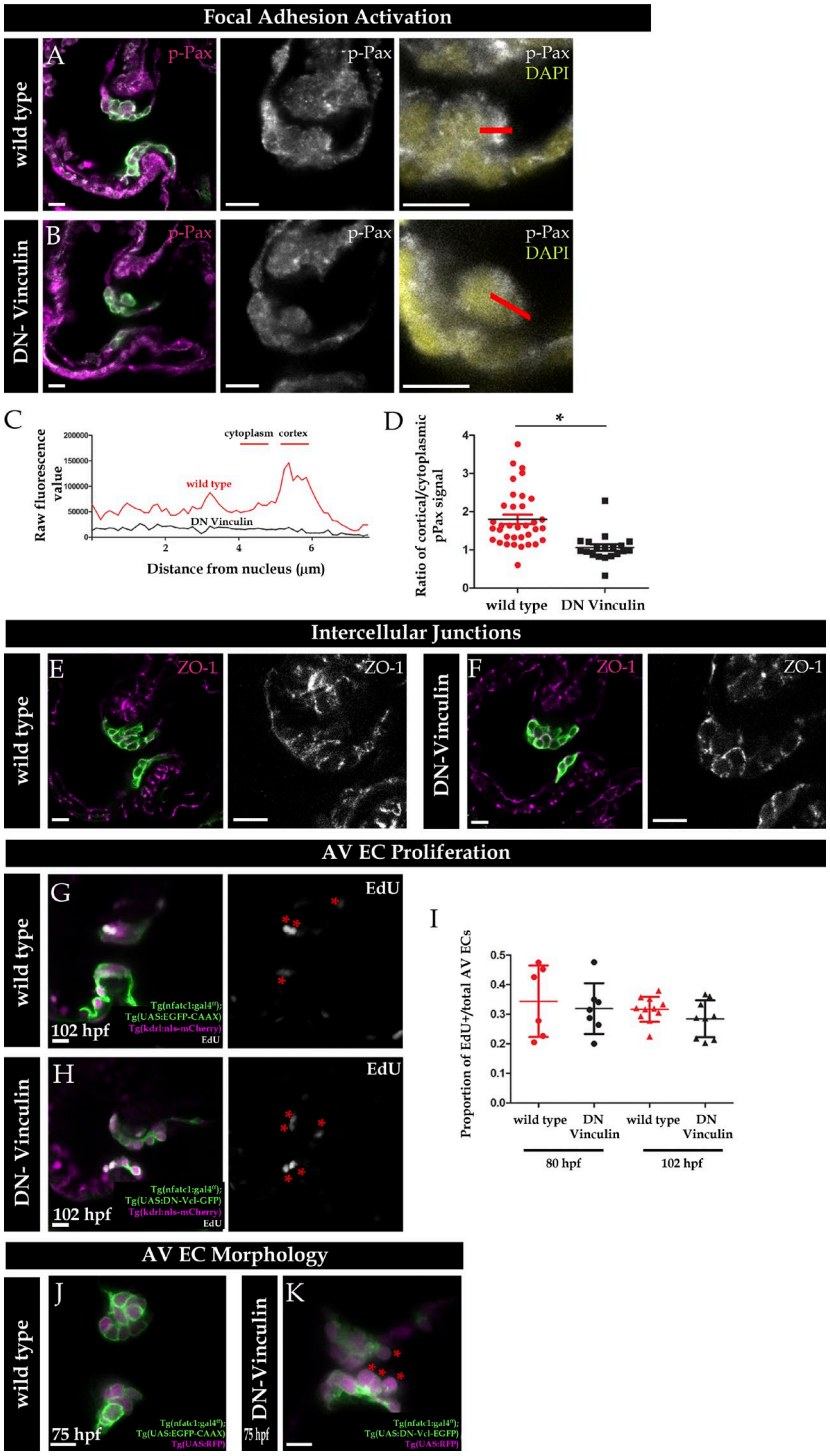

Figure S3. **The effects of DN Vinculin overexpression on AV EC behavior.** Related to Figs. 3, 4, 5, and 6. **(A and B)** Representative images of the p-Pax immunofluorescence signal in 56-hpf hearts and superior AVCs of WT (A) and DN Vinculin–overexpressing (B) animals. Red lines in right panels in A and B signify the line used to measure fluorescence intensity. **(C and D)** WT (n = 35 leader ECs/15 embryos) and DN Vinculin (n = 19 cells/11 embryos). (C) Graph shows raw fluorescence intensity values in leader ECs from one WT and one DN Vinculin overexpressing animals. The line starts from the center of the nucleus (position 0) and ends around the membrane. (D) Ratio between cortical and cytoplasmic p-Paxillin signal in the leader AV ECs. *, P = 7.43^{e-6}. **(E and F)** Representative images of the ZO-1 immunofluorescence signal in 56-hpf hearts and superior AVCs of WT (E) and DN Vinculin–overexpressing (F) animals. The signals appear similar in localization and intensity in both genotypes. **(G and H)** Representative images of AVCs in 24 h EdU-treated WT (A) and DN Vinculin–overexpressing (B) animals at 102 hpf. **(I)** Proportion of AV ECs positive for EdU compared with total number of AV ECs (as assessed by *kdrl*:nls-mCherry expression). No significant difference is observed between WT and DN Vinculin–overexpressing cells (n = 6 for WT, n = 7 for DN Vinculin, P = 0.69 at 80 hpf; n = 10 for WT, n = 9 for DN Vinculin, P = 0.21 at 104 hpf). An unpaired Student's t test was used for D and I. Error bars represent standard deviation; asterisks indicate statistical significance. **(J and K)** Representative images of AV ECs in WT, DN Vinculin–, or DN Itgβ1–expressing animals at 75 hpf. Compared with WT EC morphology (D), overexpression of DN Vinculin (E) leads to cell rounding and extrusion from the endocardial layer. Scale bars: 10 μm.

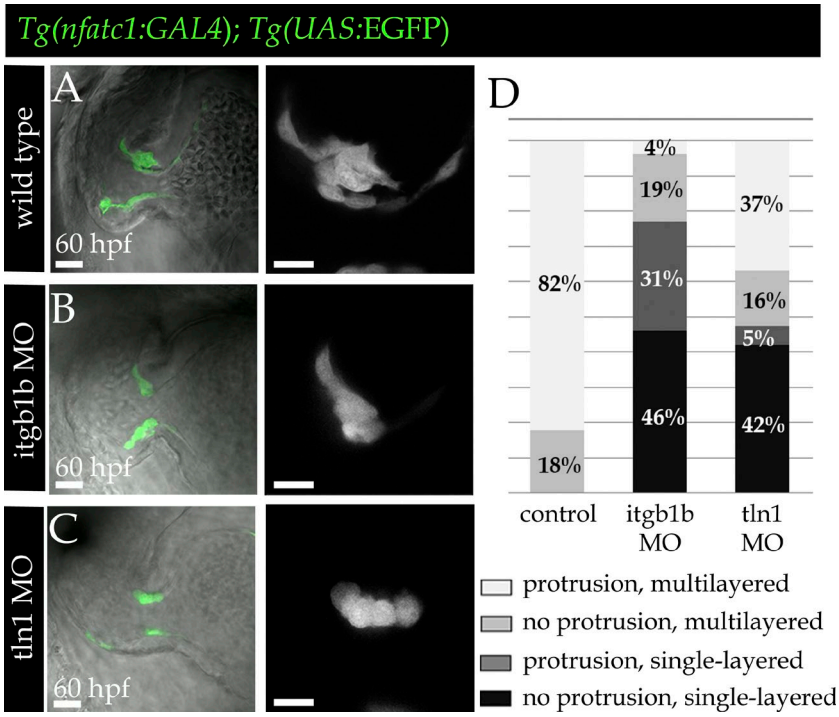

Figure S4. **Knockdown of *itgb1b* or *tln1* leads to strong delays in AV EC migration.** Related to Figs. 3 and 7. **(A–C)** Representative images of 60-hpf hearts and superior AVCs of noninjected embryos (A) and embryos injected with 0.75 ng *itgb1b* morpholino (B) or 0.5 ng *tln1* morpholino (C). **(D)** Categorization of migration stages of AV ECs (WT, $n = 17$; *itgb1b* morpholino, $n = 26$; *tln1* morpholino, $n = 19$). Knockdown of *itgb1b* or *tln1* leads to delays in AV EC migration. Scale bars: (A–C, left) 20 µm; (right) 10 µm.

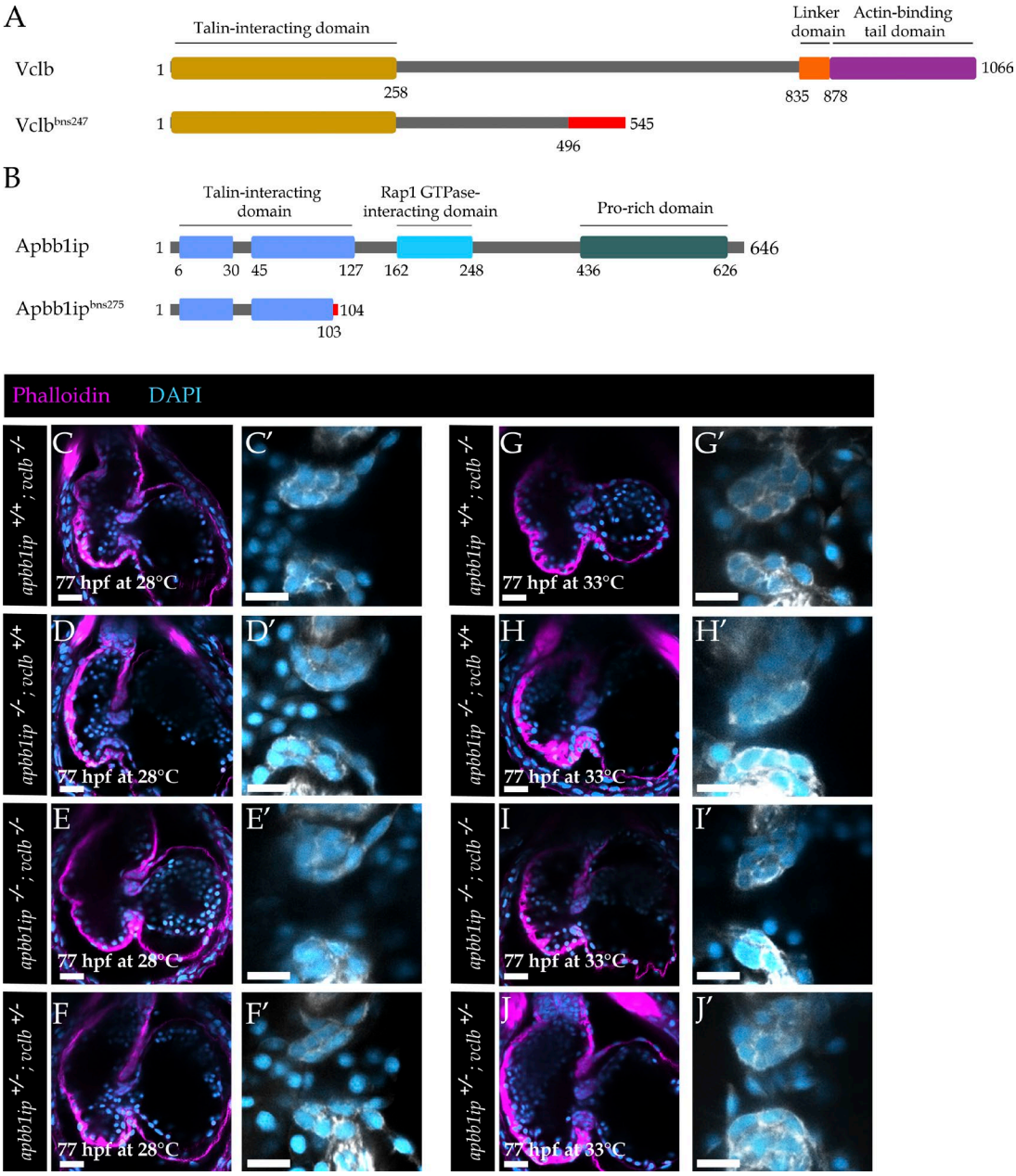

Figure S5. **Mutations in *vinculin* and *apbb1ip* do not strongly affect AV valve morphogenesis.** Related to Figs. 2 and 8. **(A and B)** Generation of mutants for *vclb* (A) and *apbb1ip* (B). Both mutations are predicted to lead to truncated proteins lacking their interaction domains with actin or actin-binding factors. Structures inferred from amino acid similarities between zebrafish and mammalian Vinculin and Apbb1ip. Red in mutant proteins indicates a new sequence downstream of the lesion. **(C–J′)** Staining with phalloidin to mark F-actin; magenta in overviews (C–J); white in magnified AVCs (C′–J′); cyan, DAPI. Analyses of 77-hpf AV valve structures when animals were raised at 28°C (C–F) or 33°C for 24 h (53–77 hpf). (C–J′) Representative images of hearts and superior AVCs of *vclb*$^{-/-}$ (C, *n* = 3; G, *n* = 4), *apbb1ip*$^{-/-}$ (D, *n* = 17; H, *n* = 11), *vclb*$^{-/-}$; *apbb1ip*$^{-/-}$ (E, *n* = 4; I, *n* = 14), and WT (F, *n* = 4; J, *n* = 4) larvae. Folded AV EC tissues observed in all genotypes examined. Scale bars: (C–J) 20 µm; (C′–J′) 10 µm.

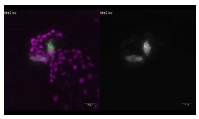

Video 1. **Real-time hourly imaging of valvulogenesis from 50 to 75 hpf in a WT animal (*Tg(nfatc1:GAL4); Tg(UAS:EGFP-CAAX)*).** Related to Fig. 4.

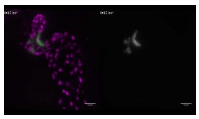

Video 2. **Real-time hourly imaging of valvulogenesis from 50 to 75 hpf in a DN Vinculin–overexpressing animal (*Tg(nfatc1:GAL4); Tg(UAS:DN-Vcl-EGFP)*).** Related to Fig. 4.

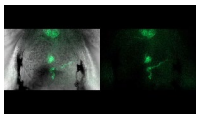

Video 3. **77-hpf beating heart of a WT larva, showing bright field and GFP.** Related to Fig. 6. The AV valve already functions at this stage, and blood flows in a unidirectional manner. AV ECs close the AVC. Video plays at 15 frames per second.

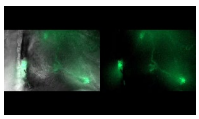

Video 4. **98-hpf beating heart of a WT larva, showing bright field and GFP.** Related to Fig. 6. Superior and inferior leaflets have formed and close the AVC upon ventricular contraction. Video plays at 15 frames per second.

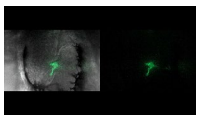

Video 5. **77-hpf beating heart of a larva expressing DN Vinculin, showing bright field and GFP.** Related to Fig. 6. Severe retrograde blood flow observed from the ventricle to the atrium. DN Vinculin–overexpressing AV ECs do not form a multilayered tissue. Video plays at 15 frames per second.

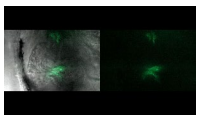

Video 6. **98-hpf beating heart of a larva expressing DN Vinculin, showing bright field and GFP.** Related to Fig. 6. Severe retrograde blood flow observed from ventricle to atrium. No AV valve leaflet structure observed when DN Vinculin is overexpressed in AV ECs. Video plays at 15 frames per second.

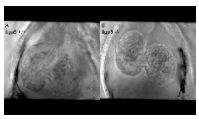

Video 7. **Representative videos of 80-hpf beating hearts of control and *itga5*$^{-/-}$ larvae.** Related to Fig. 7. A significantly higher percentage of *itga5*$^{-/-}$ larvae exhibit retrograde blood flow: 6 of 14 *itga5*$^{-/-}$ larvae (43%), compared with 1 of 7 *itga5*$^{+/+}$ (14%) and 1 of 12 *itga5*$^{+/-}$ (8%) larvae. Video plays at 15 frames per second.